A COMPARISON BETWEEN MULTI-SPECTRAL AND HYPERSPECTRAL IMAGERY FOR WATER AND AGRICULTURAL FIELDS CHANGE DETECTION USING C²VA

Alessandro Austoni – 10524152

ABSTRACT

The aim of this paper is to verify the advantages of Hyperspectral imagery with respect to Multi-spectral one, in particular by comparing change detection maps obtained by applying a C²VA algorithm. As deeper explained in section (2.2), C²VA is a very powerful technique that allows to exploit all the bands of a given data cube to perform a compressed unsupervised Change Vector Analysis. The purpose is to prove that higher spectral resolution (Hyperspectral) data can actually provide more valuable information in change detection and help detecting more changes. Because of the lack of ground truth and validation data in the studied area, the change maps comparison will be evaluated by human sight by accurately checking both RGB images and change maps, starting from expected changes in the visible spectrum. Of course, this type of approach will lead to problems mainly in the interpretation of Hyperspectral changes, that even if detected by the algorithm, will not be spotted by human sight. This, indeed, leaves room for improvement for possible following studies that will consider to integrate accurate ground truth in change validation.

1. INTRODUCTION

1.1 SATELLITES

For this study, two couples of acquisitions have been taken from the following satellites:

- PRISMA: it is a Sun-synchronous hyperspectral satellite, deployed from ASI's (Agenzia Spaziale Italiana) VEGA launch veichle. Its revisit time is 29 days with a relook of 7 days and it is a pushbroom satellite based on a prism technology. Being a hyperspectral satellite, PRISMA can cover the 400–2500 nm spectral range with 240 bands (split in 66 bands for Visible and Near Infrared cube and 174 for the Short Wave Infrared one) at a very small spectral resolution (9–13 nm VNIR and 9–14.5 nm for SWIR). Acquisitions are taken with a swath of 30km at a spatial resolution of 30m [1]. PRISMA has also an additional band, coming from a panchromatic sensor, with a higher GSD (5m), that can be used to improve the spatial resolution by the help of pansharpening techniques (those methods have not been used in this study [2]).

- Landsat 8 and 9: The Landsat 8-9 collection serves acquisitions from the two Landsat satellites (Landsat 8 and Landsat 9, the most recently launched, provided by NASA/USGS). They are both equipped with the Operational Land Imager (OLI) and the Thermal Infrared Sensor (TIRS), with 9 optical and 2 thermal bands. The main bands in the collection have a resolution of 30m, with the exception of the panchromatic and thermanl band (having respectively a resolution of 15m and 100m) (Table 1).

Bands	Wavelength (micrometers)	Resolution (meters)
Band 1 - Coastal aerosol	0.43-0.45	30
Band 2 - Blue	0.45-0.51	30
Band 3 - Green	0.53-0.59	30
Band 4 - Red	0.64-0.67	30
Band 5 - Near Infrared (NIR)	0.85-0.88	30
Band 6 - SWIR 1	1.57-1.65	30
Band 7 - SWIR 2	2.11-2.29	30
Band 8 - Panchromatic	0.50-0.68	15
Band 9 - Cirrus	1.36-1.38	30
Band 10 - Thermal Infrared (TIRS) 1	10.6-11.19	100
Band 11 - Thermal Infrared (TIRS) 2	11.50-12.51	100

Table 1 - Landsat 8 and 9 band's informations

Both Landsat 8 and 9 are pushbroom satellites, acquiring images with a swath of 185km.

The two satellites have been chosen accordingly to their different spectral resolution, with PRISMA having a much higher one (carrying 240 bands, instead of 11 for Landsat) and same spatial resolution (30m). The aim of this study is indeed to prove that an hyperspectral satellite with higher number of bands, denser in the spectrum, has a higher ability of detecting changes with an unsupervised approach. To achieve this goal it is crucial for the two satellites to have the same spatial resolution, so that the analysis can mainly evaluate changes targeting differences in the spectral resolution.

1.2 DATA PLANNING

The 4 acquisitions have been downloaded from two different portals: PRISMA images from PRISMA ASI portal and Landsat from Sentinel Hub EO Browser.

Another aim of this study is to detect droughts in the Po river, so the chosen data frames a portion of the Po river and Mincio tributary, right before their confluence, around Mantova's municipality. Detailed information about the two couples of acquisitions is reported in (Table 2).

Satellite	Acquisition Date	Central coordinates
PRISMA	2021/10/27	[45.1599, 10.7733]
PRISMA	2022/06/16	[45.1633, 10.792]
LANDSAT	2021/10/28	[45.3116, 10.5682]
LANDSAT	2022/06/16	[45.3116, 10.5682]

Table 2 - Acquisitions dates and coordinates

Due to the poor availability of already acquired images in the PRISMA catalogue, and the strict requirement of cloud free images for change detection purposes (to avoid to detect clouds as changes later in the change detection step), the two change detection dates do not trace back to the same month of the year (and season), but it was chosen the closest possible month in the following year. The same issue doesn't hold for Landsat, which has plenty of acquisitions, covering almost each day of the year, so the two Landsat images were chosen accordingly to PRISMA's availability. In each respective portal, images have been searched by looking for data with less than 40% cloud coverage.

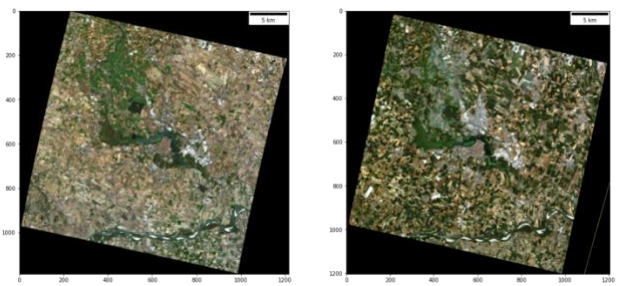

Figure 1 - PRISMA raw RGB

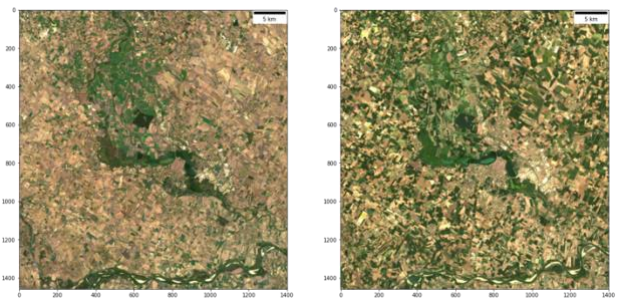

Figure 2 - Landsat raw RGB

By looking to the swaths of the two satellites, it is clear that the multispectral satellite (Landsat) is acquiring images framing a larger land portion. Since the two couples of acquisitions have been requested by different portals, the PRISMA acquisition contains a complete tile of 30x30km² (PRISMA portal doesn't allow to crop a specific tile, but the full one must be downloaded), while the Landsat one have been cropped to a specific area of interest (thanks to the tools offered by EO Browser).

1.3 EXPECTED CHANGES

The main changes expected, as can be deduced from the RGB couples (Figure 1 – Figure 2), are the agricultural field's ones: many fields appear to be "greener" in latter (October) acquisitions, probably due to different use of the land accordingly to the season or thanks to a more watered landmass. In addition to that, also shallows in the Po river (or Mincio tributary) are expected, due to the dry period that the river is going through during 2022; this is also noticeable from a first sight of the raw acquisitions, as some of the white zones inside the Po river (exposed rocks from the river's bed, in the south-east of the image), appear to engage a larger area in the second acquisition.

1.4 DATA PRE-PROCESSING

After downloading the acquisitions from PRISMA portal at their highest processing level (L2D), the data have been first accessed in the HDF5 (Hierarchical Data Format) format and then copied inside two different data cubes (a Numpy stack of the different bands stacked along the third dimension, one for VNIR and another for SWIR) and then pre-processed in order to transform the raw information into reflectance values, following the procedure explained in PRISMA manual [3].

Data supplied from EO browser website, instead, is Level-2 data that already provides reflectance values, so it doesn't need further processing. Bands provided from the website are respectively: 01, 02, 03, 04, 05, 06, 07, 10. In order to keep the same spatial resolution for all the bands, band number 10 (thermal) has been removed from the Landsat data cube, because the lower resolution (100m) would have compromised the analysis of the study.

1.5 CODE REPOSITORY

The link to the full code repository can be found on Github at the following link: https://github.com/AlessandroAustoni/EO, a complete explaination of the code arrangement can be retrieved in the 'README.TXT' file)

2. MATERIALS AND METHODS

2.1 COREGISTRATION

Coregistration is a fundamental task in remote sensing, especially in change detection, because it allows images to be perfectly overlapped and matching each other. Thanks to this, change detection can benefit from the procedure, by reducing the number of 'false positives' (changes detected by the misalignment of the two images).

Although accordingly to [4], PRISMA L2D data is already geocoded and orthorectified, the lack of PRISMA Ground Control Points, causes the coregistration accuracy to reach a very low level, where images from the same sensor in different time instants are shifted in the order of 2-3 pixels (sometimes, in some of the worst scenarios, even of 5-8 pixels). This, considering a GSD of 30m, is not acceptable for Change Detection, since the misalignment error would propagate into this further step.

The same doesn't holds for Landsat, which has a strong network of GCP's, that are used for Level-2 data.

To achieve a good coregistration without relying on GCP's, it was chosen to use the Gefolki algorithm (Github repository can

be found here: https://github.com/aplyer/gefolki), which is a non-parametric approach, that relies on pixel intensity correlation.
The algorithm is, indeed, an adaptation of one of the most common optical flow approaches, the gradient based Lukas Kanade algorithm, from which it is derived with the addition of some modifications.

The starting point is the typical optical flow equation, given two 2-D images (I_1 and I_2), a window ω, which is typically a square (parameterized by its radius $(2r + 1) \times (2r + 1)$) and a displacement u(x) (where x represents the coordinates of the window center):

$$J(u;x) = \sum_{x'} \omega(x' - x)(I_1(x') - I_2(x' + u(x))^2 \qquad (1)$$

Then, two main modifications are introduced, first the addition of a rank function R(I) to compress the signal dynamics:

$$J(u;x) = \sum_{x'} \omega(x - x)(R(I_1)(x) - R(I_2)(x + u(x))^2 \quad (2)$$

The last modification is the variation of the window size ω, in order to take into account of different pyramid levels to look for larger displacements during the iterative procedure [5] [6].

For the algorithm to converge, it is necessary to go through a first initialization step. This step requires that the two acquisitions are cropped almost to the same area of interest. Although this feature is already included in most of satellite images providers like the EO Browser, used for Landsat data in this study, the same cannot be stated for PRISMA acquisitions, which are provided in the form of entire tiles, that have just a common intersection, that should be then manually extracted by the user with other tools (for this study, it was created a proper function in python exploiting Latitude and Longitude metadata provided in HDF5 format) (a visual representation in Figure 3).

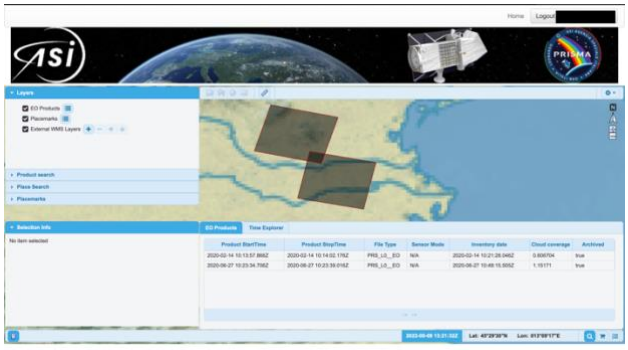

Figure 3 - tile intersection in PRISMA portal

After the initialization step, a reference image and a matching one must be chosen, so that Gefolki will estimate the transformation to be applied to the matching one, taking the first as reference. After computing the transformation (applied with a simple function call) the shifts from one image to the other one are returned in the form of two matrices: horizontal shifts and vertical ones (known as 'u' and 'v'). Each value inside the matrix represents a pixel shift along a certain direction (horizontal or vertical). Finally, another function call (using the matching image as input parameter) will modify the image content with shift information, to match the reference image. In particular the flow is computed through an iterative process, in which a fixed length window (ω) cycles through the two images and looks for correlation between the two windows, by going through different pyramid levels.
In this specific study, PRISMA data have been coregistered separately from Landsat and vice versa, since the aim of this step is just to avoid misalignments in CD step and not to have perfectly overlapped change maps (which even if not aligned can be compared by human sight to search for detected feature from PRISMA or Landsat).
A more complete list of Gefolki's input parameters can be found at [9].
In particular the following ones are the parameters that worked best for this analysis (both for PRISMA and Landsat acquisitions):

- window radius (r) along both x and y: 70 pixels
- number of iterations: 8
- size of the rank filtering: 4
- pyramid levels: 5.

2.2 C²VA (CHANGE VECTOR ANALYSIS)

Compressed change vector analysis is a change detection procedure, that allows to detect changes in an unsupervised way, from two images taken at different times, by exploiting the content of all the bands in a satellite image cube (where the band is the third dimension).
The output of this process is the same of the classical CVA: a magnitude and an angle matrix (more information on CVA can be found here [7]).
C²VA magnitude can be computed through the following formula [8]:

$$X_\rho = \sqrt{\sum_{b=1}^{B} X^2{}_{b,D}} = \sqrt{\sum_{b=1}^{B} (X_{b,2} - X_{b,1})^2} \qquad (3)$$

Where:
- B: maximum band number
- X_b: single band image (at band 'b')

While the angle, can be obtained, by using a reference unit vector $X_{ref} = \left[\frac{\sqrt{B}}{B}, \dots, \frac{\sqrt{B}}{B}\right]$ in the following way:

$$X_\alpha = arcos\left(\frac{\sum_{b=1}^{B} X_{b,D} X_{b,D}}{\sqrt{\sum_{b=1}^{B} X_{b,D}^2 \sum_{b=1}^{B} X_{b,ref}^2}}\right) \qquad \alpha \in [0,\pi] \qquad (4)$$

Although magnitude has the same meaning of CVA one (stating the entity of the change, higher the value, greater the change), angle has a totally different meaning.
To better understand this concept, the most used representation on this field is the polar one, in which each point represents a single pixel, and its coordinates are given by its radius and angle.
In Figure 4 it is reported an example of CVA and C²VA polar representation.

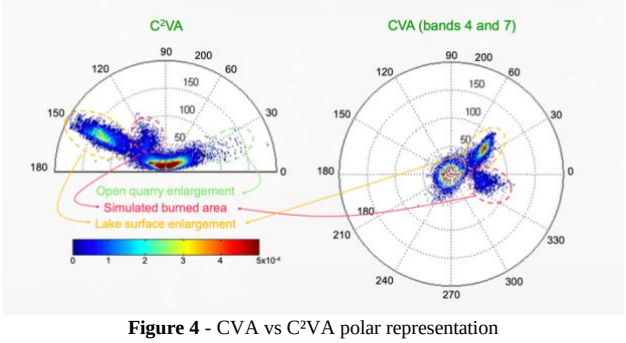

Figure 4 - CVA vs C²VA polar representation

In both cases the radius acts as change magnitude, the further the pixel from the coordinate center, the greater the amount of change (a threshold can be set in the radius, to split in 'changed' and 'not changed' pixels). What makes C²VA different is, instead, the angle: first of all, C²VA has a maximum angle of 180° (differently from the 360° of CVA). In addition to that CVA

only uses two bands, so the angle will just state whether one change is attributable to increase or decrease of one band or the other.
Moreover, bands should be accurately chosen accordingly to the expected change, and this requires some prior knowledge of changes themselves, which is not always available.
On the other side, C²VA angle allows for a more sophisticated interpretation, accordingly to which the different angles assumed by each pixel will most likely help to cluster pixels in groups, and so to classify changes in an unsupervised manner (another threshold can be set by the angle to define the k-th annular sector, representing the k-th change type/class).
In addition to that, being this a "compressed" technique, all the bands will be considered in the study, allowing acquisitions to exploit the full content stored in one image.
Although this may seem a very important advantage, it must be remembered that the angle interpretation in this field is still very controversial, and in addition to that, even if at first glance it may seem that hyperspectral data will benefit more than multispectral from C²VA thanks to its numerous amount of bands, allowing to detect more changes, it is also true that the high spectral resolution may lead pixels to be really close to one another (finer changes due to close angle values), leading to less clustering and harder interpretation of the polar graph.
On this purpose, some studies have proven that multispectral data has a greater ability of clustering in C²VA [8].
In the following paragraph, Hyperspectral and Multispectral C²VA results, have been summarized to prove that they meet the aforementioned expectations.

3. RESULTS DISCUSSION

For coregistration it will be illustrated a list of the results obtained from the analysis (section 3.1 and 3.2), in the form of:

- Optical flow shift's norm (graph): this graph shows the intensity of the computed shift (at the pixel scale), from the Gefolki algorithm, to be applied to the matching image. X and Y axis corresponds to the pixel index in the image. The norm is obtained by the following formula:
  $N = \sqrt{u^2 + v^2}$ (5)
  Where:
  - u: horizontal shift matrix
  - v: vertical shift matrix
- Norm histogram distribution: the probability distribution of the aforementioned norm. X axis corresponds to the shift pixel value and Y axis to its frequency
- Image overlay: this is an image representation in which usual RGB channels are substituted with the grey scale matrices of two RGB images acquired at different time instants (October 2021 and June 2022), in the following form:
  $[R, G, B] = [Grey_2, Grey_1, Grey_2]$ (6)
  Where:
  - $Grey_1$: grey scale matrix derived from first acquisition in time
  - $Grey_2$: grey scale matrix derived from second acquisition in time

  This representation is shown before and after coregistration, so that it will be possible to appreciate its effects on the image after the process (if noticeable). Violet features will correspond to the second acquisition (Red and Blue channel), while green one to the first acquisition (Green channel).

CD results (section 3.3 and 3.4) are listed in the following form:

- Magnitude map: showing the intensity value of C²VA changes computed as in (3)
- Binary map (change map): obtained by labelling as 'change' pixel values exceeding the 80 percentile of the magnitude map, and 'no change' the remaining ones.
- Angle map: angle value computed as in (4) for each pixel, stating, accordingly to the literature, the type of change.
- Polar graph: polar representation using radius (as magnitude (3)) and angle (as angle (4)) coordinates.

Change maps are specific square areas, extracted from both PRISMA and Landsat full acquisitions, as 450x450 pixel windows, obtained by a function that crops the two images, given the coordinates of the top left square corner. The studied area for CD is shown in Figure 5.

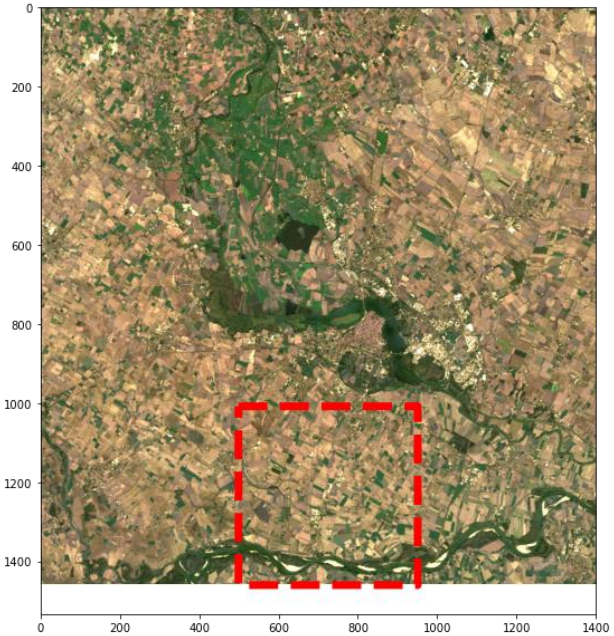

Figure 5 - CD studied area

3.1 COREGISTRATION (LANDSAT)

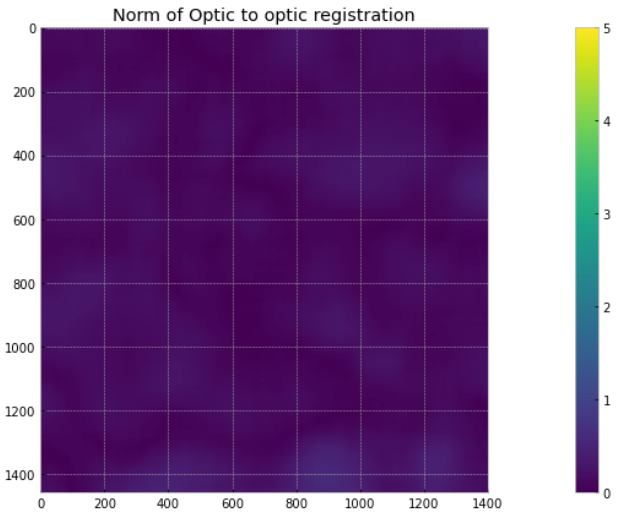

Figure 6 – Landsat optical flow shift's norm

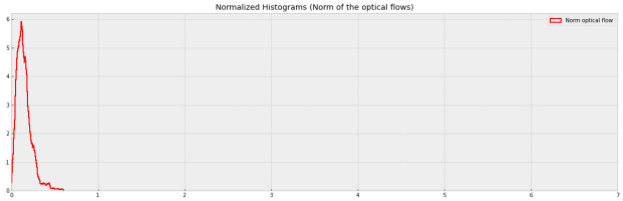

Figure 7 – Landsat optical flow shift's norm (histogram distribution)

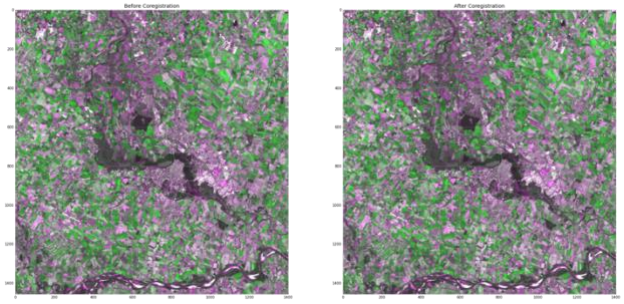

Figure 8 - Landsat before and after coregistration image overlay

As evicted from Figure 6 and Figure 7, coregistration shifts to be applied to the second acquisition are under the pixel level (the greatest shift detected is around 0.5 pixels). This proofs that Landsat Level-2 acquisitions are already accurately coregistered, and no further coregistration is needed.
Also the image overlay (Figure 8) is not showing any difference before and after the procedure.

3.2 COREGISTRATION (PRISMA)

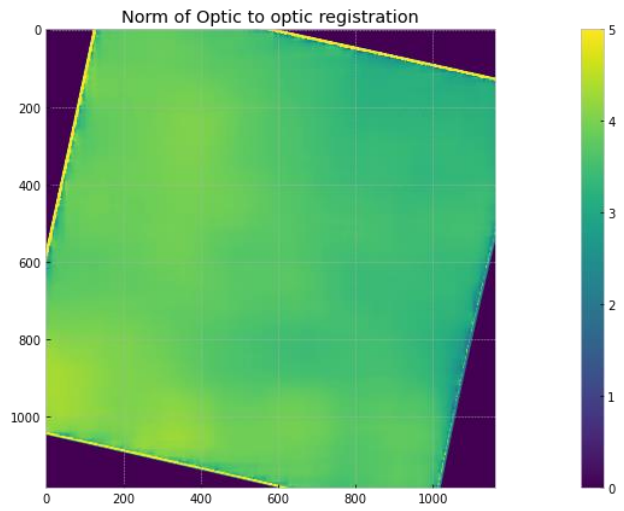

Figure 9 – PRISMA optical flow shift's norm

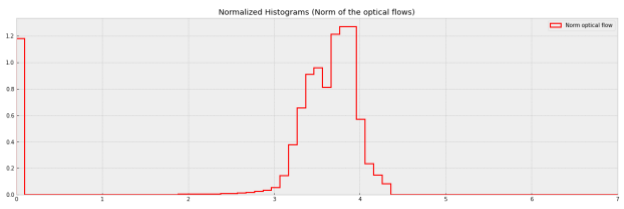

Figure 10 - PRISMA optical flow shift's norm (histogram distribution)

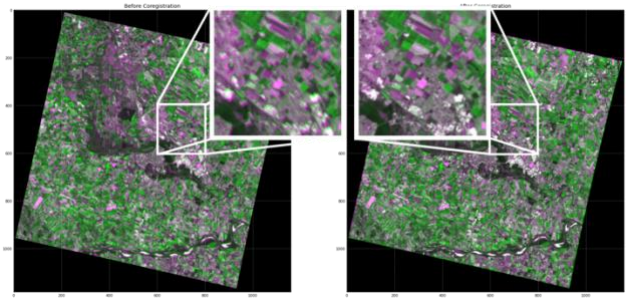

Figure 11 - PRISMA before and after coregistration image overlay

A completely different analysis should be done for PRISMA acquisitions. Shifts are larger with respect to Landsat ones, reaching in particular a maximum around 4.5 pixels (Figure 10). The image overlay (Figure 11) is clearly showing a misalignment of the two acquisitions before the coregistration, which clearly appear to be fixed after the process (the zoom distinctly shows that before coregistration the overlay of the two images appear "out of focus": fields and urban buildings are misaligned).

3.3 C²VA (LANDAST)

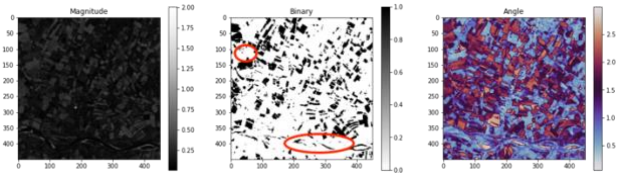

Figure 12 - Landsat magnitude, binary and angle map

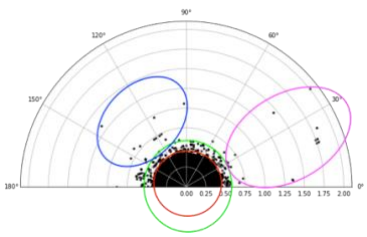

Figure 13 - Landsat polar plot

The binary change map (Figure 12) is proving that Landsat is correctly able to detect changes in agricultural fields and changes in the river. As anticipated in section 1.3, not only fields are changing, but even some white rocks in the bed of the river are exposed to sun light, showing clear shallows in the river, which are correctly detected by the algorithm (red circle at the bottom of Figure 12).
In the polar plot (Figure 13) a proper threshold can be effectively chosen (red circle) by setting a proper radius value, splitting data in 'change' and 'no change', and another threshold of more 'subtle changes' can be clearly drawn (green circle).
On the other side, the polar plot clustering is not as much clear as expected from multispectral imagery in literature [8], but at least two main clusters can be highlighted in the graph (blue and purple circle). What is mainly hard to infer is the type/class of change that can be assigned to those two main clusters and this is the first weakness of this unsupervised technique (river and field changes can be a first guess, but there is no way to validate that this choice is the correct one).

3.4 C²VA (PRISMA)

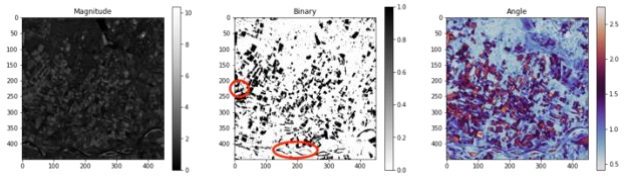

Figure 14 - PRISMA magnitude, binary and angle map

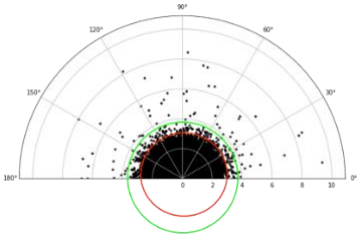

Figure 15 - PRISMA polar plot

On the contrary, PRISMA is detecting more changes in the binary map with respect to the ones detected by Landsat. PRISMA is, indeed, detecting more shallows in the Po river (red circle at the bottom of Figure 14 and Figure 12), and also inland changes (red circle at the top left of Figure 14 and Figure 12, probably a white plastic field cover visible in the second RGB acquisition).
However, as expected from literature [8], the higher sensibility of hyperspectral imagery in detecting changes, leads to a more complicated interpretation. Indeed, even if in the polar plot (Figure 15) a proper threshold can be set for 'no changes' (red circle) and 'subtle changes' (green circle), pixels are too close to one another to precisely define a cluster in the change region.

3.5 CONCLUSIONS

In conclusion, these final results are showing that, not always having more information means achieving better results. The enormous amount of bands provided by PRISMA surely have a greater potential with respect to multispectral data, especially in detecting changes that are not always visible by human sight, but more processing and effort needs to be put in place to have a clear interpretation of those results.
Not only changes that are not visible by human sight, are hard to be validated (if, like in this case, there is no ground truth) and add complexity to C²VA clustering, but at the same time C²VA in general exposes a common issue also to multispectral data: how to assign labels to clusters?
This confirms the idea, that C²VA is a powerful unsupervised change detection technique, that however, needs to be integrated and supported by more accurate analyses, like classical CVA (by choosing properly two specific bands contributing to the sought change).
Hoping that this could be the starting point for further developments and studies that are willing to follow this path, a list of improvements that will possibly enhance the differences between hyperspectral and multispectral imagery, are reported down below:

- As can be evicted from Figure 12 and 14, Landsat and PRISMA change maps are not perfectly overlapped, and this is due to the manual cropping (performed by a human, through a function that subset the image given proper pixel coordinates) that has been performed on coregistered pairs, in order to have an approximate close study area in images taken from the two different sensors. A possible way of improving the comparison and alignment of PRISMA and Landsat acquisitions, can be to apply the Gefolki algorithm after the manual cropping of the acquisitions, in order to coregister not only images at different time instants, but also from different sensors.
- Select use cases with a higher number of change classes: in this region (Mantova), changes are mainly caused by water variation, for both fields and river. By considering a different location, with a higher number of changes, it would be probably possible to appreciate a higher number of clusters in the C²VA procedure
- Validate results taking advantage of an accurate ground truth (especially for binary change maps and change class labels), instead of relying on human sight comparisons. In this study this was not possible due to lack of ground truth in the studied area.
- Experiment further C²VA variants in literature, which purpose is to enhance pixel clustering [8].

4. REFERENCES

[1] The PRISMA imaging spectroscopy mission: overview and first performance analysis *S. Cogliati, F. Sarti, L. Chiarantini, M. Cosi, R. Lorusso, E. Lopinto, F. Miglietta, L. Genesio, L. Guanter, A. Damm, S. Perez-Lpez, D. Scheffler, G. Tagliabue C. Panigada, U. Rascher, T.P.F. Dowling, C. Giardino, R. Colombo*

[2] Pansharpening PRISMA Data for Marine Plastic Litter Detection Using Plastic Indexes *Maria Kremezi , Viktoria Kristollari , Vassilia Karathanassi , Konstantinos Topouzelis, (Member, IEEE), Pol Kolokoussis , Nicolò Taggio, Antonello Aiello , Giulio Ceriola, Enrico Barbone, Paolo corradi*

[3]http://prisma.asi.it/missionselect/docs/PRISMA%20Product%20Specifications_Is2_3.pdf

[4] The New Hyperspectral Satellite PRISMA: Imagery for Forest Types Discrimination *Elia Vangi 1,2, Giovanni D'Amico 1, Saverio Francin*

[5] Adaptation and Evaluation of an Optical Flow Method Applied to Coregistration of Forest Remote Sensing Images *Guillaume Brigot, Elise Colin-Koeniguer, Aurelien Plyer, and Fabrice Janez*

[6] A New Coregistration Algorithm for Recent Applications on Urban SAR Images *Aurélien Plyer, Elise Colin-Koeniguer, and Flora Weissgerber*

[7] A Theoretical Framework for Unsupervised Change Detection Based on Change Vector Analysis in the Polar Domain *Francesca Bovolo, Student Member, IEEE, and Lorenzo Bruzzone, Senior Member, IEEE*

[8] Advanced Techniques for Automatic Change Detection in Multitemporal Hyperspectral Images *Sicong Liu*

[9]https://github.com/aplyer/gefolki/blob/master/manual_gefolki_english.pdf